Article

A Comprehensive and Sustainable Recycling Process for Different Types of Blended End-of-Life Solar Panels: Leaching and Recovery of Valuable Base and Precious Metals and/or Elements

Maryam Kavousi and Eskandar Keshavarz Alamdari *

Department of Materials and Metallurgical Engineering, Amirkabir University of Technology
(Tehran Polytechnic), Tehran 15875-4413, Iran; maryamkavousi1989@gmail.com
* Correspondence: alamdari@aut.ac.ir; Tel.: +98-216-454-2971

Abstract: The production of photovoltaic modules is increasing to reduce greenhouse gas emissions. However, this results in a significant amount of waste at the end of their lifespan. Therefore, recycling these solar panels is important for environmental and economic reasons. However, collecting and separating crystalline silicon, cadmium telluride, and copper–indium–gallium–selenide panels can be challenging, especially in underdeveloped countries. The innovation in this work is the development of a process to recycle all solar panel waste. The dissolution of all metals through the leaching process is studied as the main step of the flowchart. In the first step of leaching, 98% of silver can be recovered by 0.5 M nitric acid. Then, the second and third step involves the use of glycine for base metal dissolution, followed by the leaching of valuable metals with hydrochloric acid. The effect of parameters such as the initial pH, acid concentration, solid/liquid ratio, and hydrogen peroxide concentration is studied. The results show that up to 100% of Cu, Pb, Sn, Zn, Cd, In, Ga, and Se can be recovered under optimal conditions. The optimal conditions for the dissolution of Cu, Zn, and Cd were a glycine concentration of 0.5 M, a temperature of 25 °C, a solid/liquid ratio of 10 gr/L, and 1% of hydrogen peroxide. The optimized glycine concentration for the leaching of lead and tin was 1.5 M. Indium and gallium were recovered at 100% by the use of 5 M hydrochloric acid, S/L ratio = 10 gr/L, and T = 45 °C. Separation of selenium and tellurium occurred using 0.5 M HCl at a temperature of 60 °C. Additionally, for the first time, a general outlook for the recycling of various end-of-life solar panels is suggested.

Keywords: solar panel recycling; leaching; base metals: precious metals; waste management; environmental impact; sustainable technology

1. Introduction

In recent years, solar panels have played a significant role in reducing global warming by generating clean and emission-free electricity from the sun, thus reducing the reliance on greenhouse-gas-producing fossil fuels [1]. Solar energy is considered the fuel of the future due to its potential for meeting increasing electricity demand and reducing greenhouse gas emissions. As a result, the mass production of solar panels using different technologies has increased in recent decades, and the production of new generations of solar panels is expected to continue [1,2]. However, despite the positive impact of solar panels, their production also has negative consequences, including the generation of large amounts of waste. The average lifetime of a PV panel is 25 years, and, given their worldwide production, it is anticipated that there will be a significant amount of waste generated annually. According to the International Renewable Energy Agency (IRENA) report, apart from considering the generation of a large amount of waste during the manufacturing process of solar cells [3,4], an estimated 80 million tons of PV waste will be generated by 2050 [5].

The issue of solar panel waste is significant from two perspectives. Firstly, these wastes contain lead, cadmium, and other harmful chemicals that can cause significant health and environmental hazards [6,7]. Secondly, these wastes are considered valuable due to their high content of valuable metals [7–10]. Therefore, the life cycle assessment (LCA) should be applied to evaluate all aspects of the environmental impacts, energy consumption and production, and emissions during the entire life cycle of solar panel technology. LCA is a feasible method that can be used as an environmental management tool to consider the positive ecological effects of solar panels due to the decrease in carbon emissions and energy consumption. This should also be used to evaluate the potential cradle-to-grave life cycle impacts of solar panels after their service life, as it is uncertain what will happen to this massive amount of solar panel waste.

Although few LCA studies have explored the recycling of PV technologies, some have investigated the production and use of PV technologies [11,12] and the energy consumption due to PV recycling [13]. The main factors affecting end-of-life panels' waste management are self-take-back collection, recycling facilities, and material recovery [14].

The most commonly used PV panels are crystalline silicon and thin-film PV cells. The former accounts for around 80% of the market share, but this is decreasing due to their increased capacity and the reduction in production costs [15]. Conversely, the lower production costs and optimum efficiency of thin-film panels are driving their growth in the overall photovoltaic market [15–17]. However, the handling and waste management of this extensive range of used solar panels that contain Cd, Se, Pb, and other environmentally hazardous metals pose an environmental concern. Additionally, there is another concern about the fate of these sources of valuable metals. These two perspectives will soon force industries and governments to plan for the safe disposal or recycling of PV waste.

Although many researchers have studied the recycling processes of used solar panels [18–24], only two processes have been established on an industrial scale. The recycling of C-Si and CdTe thin-film modules is operated by Deutsche Solar and First Solar, respectively [25–27]. The first step in the recycling process is the separation of the modules, followed by the separation of the non-metal and metal parts. Many separation methods have been developed for C-Si [28–31], CdTe [32–34], and copper–indium–gallium–selenide (CIGS) [18,35,36], most of which include physical, mechanical, and chemical processes. This step involves the elimination of glass, Al, and plastic, as well as the separation of metal and non-metal parts from solar panels. Other recycling processes are different for different types of solar panels. The recycling processes for silicon solar modules typically involve delamination and metal extraction. The solar cell electrodes and interconnected ribbons, made of silver, aluminum, and copper, are dissolved in aqueous media for recycling [37,38]. Two of the most advanced processes developed worldwide are the Full Recovery End-of-Life Photovoltaic (FRELP) and Baseline processes [39].

The recovery of cadmium and tellurium from cadmium telluride PVs is difficult due to their low content in the semiconductor [40]. There are many hydrometallurgical recycling processes for CdTe, as well as acid dissolution and subsequent precipitation [41], cementation [42], electroplating [43], and ion exchange [44,45]. A recycling process for CdTe PVs based on a sequence of mechanical steps rather than wet-chemical techniques has also been proposed [46].

In recent years, researchers have shown significant interest in end-of-life CIGS panels due to the presence of gallium and indium [47,48]. Several recycling processes, such as mechanical techniques [49], wet-chemical processes [50], electrochemical methods [51], and the leaching and electrolyzing of metals, have been developed [52]. Xiang Li and colleagues have reported an effective separation process by using an alkaline agent [53]. They found that selective alkali leaching is feasible for separating indium and gallium effectively into pure In_2O_3 and Ga_2O_3, respectively. The recycling of copper, indium, and gallium from thin-film solar panels has also been reported [54], where H_2SO_4 is used as a leaching agent. In many studies, the separation of indium and gallium was studied by solvent extraction and ion exchange following the leaching step [55].

On the topic of recycling, an important point is that using a single treatment or recycling process is not usually practical for recycling all the waste of a particular type [56]. Given the variety of solar panels on the market and the need for economically feasible recycling processes, the recovery of metals through the co-processing of all types of solar panels was examined by a comprehensive and innovative approach in this study. To do this, the metallic and non-metallic parts from Si, CdTe, and CIGS solar panels were separated and subjected to hydrometallurgical processes. This is the initial step of the suggested flowsheet and includes the separation of metallic and non-metallic parts and comprehensive leaching studies of copper and other base metals. Copper is the main component of solar PV systems due to its thermal and electrical conductivity, but other base metals are also used in solar PV systems. Many hydrometallurgical methods have been studied for the dissolution of copper and other base metals; most of these studies used two or more leaching agents in two or more stages [57–61]. The simultaneous leaching of copper and solder alloy was studied by a new method from PCB waste, with HBF_4 as the leaching agent [62]. After the leaching step, there were different methods for the separation of copper from other metals, including solvent extraction [62–66], precipitation [67,68], and cementation [69]. In the second step of our approach, the recovery of gallium and indium by chemical leaching has been proposed. The optimum conditions for the selective extraction of copper, the further leaching step of other base metals, and the extraction of indium and gallium have been investigated.

By utilizing glycine amino acid, an eco-friendly leaching agent, in the initial step of the process, this recycling method is not only environmentally friendly but also economically feasible. In many studies, the leaching of base metals has been successfully conducted by glycine as a dissolution agent [70–73]. The study also provides insights into the leaching behavior of various metals under different conditions, allowing for the selective extraction of different metals from solar panels. Furthermore, the paper presents a general flowsheet for the recycling of all types of solar panels, which has the potential to be implemented globally in the future, considering its economic and environmental benefits. The study highlights the importance of developing comprehensive recycling methods for spent solar panels to ensure the effectiveness of solar PV technology and to reduce its environmental impact. It is hoped that this approach will be a significant contribution to the field of solar panel recycling, and it can potentially pave the way for future research and development in this area.

2. Materials and Methods

2.1. Material and Reagents

To conduct the research, a variety of C-Si, CIGS, and CdTe solar panels, including alloy layers such as CdTe and CIGS, were collected. While thin-film solar panel technology has not yet been established in Iran, the collection of these materials allowed for the development of a new route for recycling all kinds of solar panels in a single plant. The metallic parts were separated from other parts through physical processing and thermal treatment [34], making it economically and environmentally feasible to recycle all metals from different types of photovoltaic panels through the same continuous process route. Analytical-grade nitric acid (65%) for the leaching of silver, glycine (50%) for the leaching of base metals, hydrochloric acid (37%) for the valuable metal leaching, hydrogen peroxide (30 wt.%) as oxidant, and ammonia (25%) for the increasing of pH were purchased from Merck Chemicals Company. All aqueous solutions were prepared using distilled water.

2.2. Initial Preparation of Samples from Different Types of Solar Panels

Although the composition of solar panels can be different due to the different manufacturers and rapid changes in the innovations of technology, the common multi-layered structure of all PV panels, which includes glass and a polymeric matrix (EVA, PVF, or Tedlar), has been considered in the preparation step. The preparation step for different kinds of PV panels begins with the shredding process after the manual dismantling of

the Al frame. This step is followed by gravitational separation, magnetic separation, and thermal treatment, in accordance with previous research [22,29,32,35]. The PV panels were cut into small pieces of 10 * 10 cm via a cutting machine. These pieces were shredded to ≤1 mm by an SM-2000 cutting mill (Retsch, Haan, Germany) and sieved into different fractions using standard sieves. The majority of the glass was recovered in the fraction of >1 mm. Also, the EVA was completely removed after thermal treatment at 700 °C [74,75]. The solid feed material in the leaching process was ≤1 mm. As shown in Table 1, this sample includes many components, including BMs, PMs, and other valuable metals.

Table 1. The XRF results of the major metal contents of the sample with the size of ≤1 mm (prepared in this study by using end-of-life solar panels and alloy layers).

	Cu	Pb	Sn	Cd	Zn	Ag	Se	In	Ga	Te
Metal content (Wt.%)	38	1.9	1.1	0.81	5.9	0.56	0.12	0.09	0.08	0.51

2.3. Methods

All leaching experiments were carried out in a 1 L autoclave equipped with a mechanical stirrer, a reaction-temperature control unit (298–313 K (25–80 °C)), and a condenser to avoid loss of solution (Figure 1). The initial pH value was adjusted to a preset value by carefully adding ammonia solution, and the acidity of the solution was measured using a Mettler Toledo SevenExcellence S400 pH Meter. The agitation was fixed at 300 rpm. At the end of the leaching time, the slurry was filtered, and the obtained filtrate was delivered to the analyzing step.
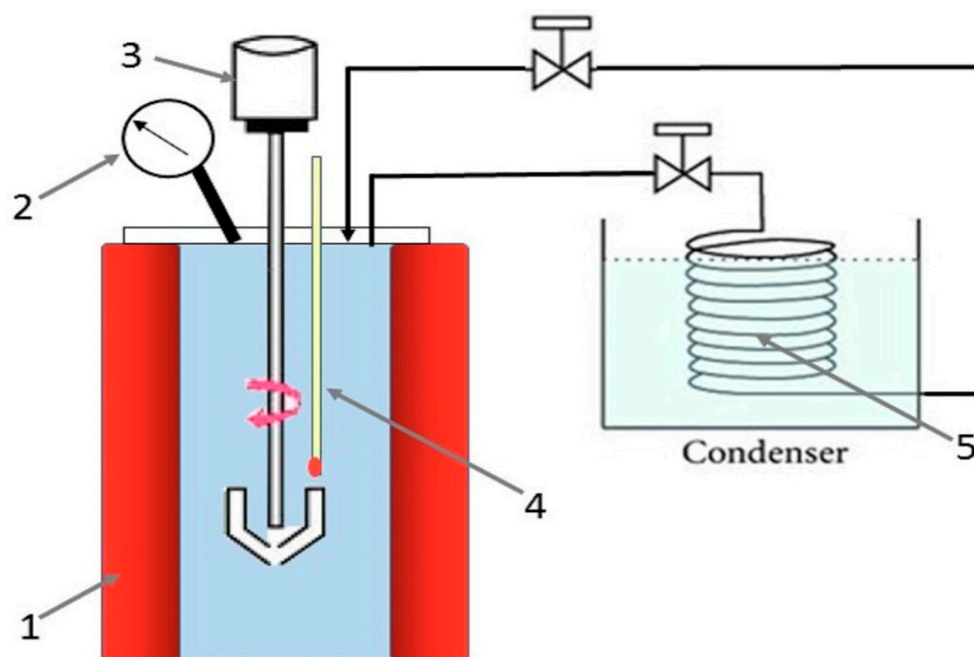

Figure 1. Schematic diagram of the lab-scale autoclave reactor: 1—Electric heater; 2—Pressure sensor; 3—Stirrer; 4—Temperature sensor; 5—Condenser.

In the first step, 0.5 M diluted nitric acid was used to leach the samples and to recover silver. The goal of this step is the selective extraction of silver over other metals. Many researchers have found that HNO_3 shows good performance in the selective dissolution of silver over tin and lead [29,76–78]. After leaching, the samples were filtered and dried; subsequently, leaching experiments were conducted with glycine. To determine their impact on the leaching efficiency of base metals, the effects of glycine concentration, initial pH value, H_2O_2 volume concentration, time, and liquid-to-solid ratio were evaluated. The

experimental conditions were based on the potential–pH diagrams of the copper–glycine system at 25 °C and 1 atm, as described in a study by Serdar Aksu and Fiona M. Doyle [79]. After glycine leaching, the raffinate was subjected to the next experiments. The residue solid was prepared as the feed material for the next leaching step by roasting. In the final leaching step, HCl was used as the leaching agent, and the leachate from the leaching step was analyzed for the measurement of the extraction rate. The effect of the liquid-to-solid ratio, acid concentration, temperature, and pH was studied as the affecting parameters on the second leaching step.

2.4. Multivariate Design of Experiment

The aim of this study is the development of a complete and innovative flowsheet for the co-processing of all types of solar panels. To achieve that, the procedure of optimizing the leaching operating parameters via the response surface methodology (RSM) is employed. A Box–Behnken design was utilized to investigate the influence of the four factors on the recovery of Cu, Zn, Cd, Pb, and Sn, respectively. The study comprised 28 experimental runs using the response surface methodology (RSM) and Design Expert 13. The design includes one block and four central points for each block. The numerical factors considered in the study were the glycine acid concentration, solid/liquid ratio, initial pH, and H_2O_2 dosage, coded between −1 and +1, as shown in Table 2.

Table 2. Factors and their levels.

Factor	Name	Unit	Minimum	Maximum	Coded Low	Coded High
A	[GLY]	M	0.10	1.50	$-1 \leftrightarrow 0.10$	$+1 \leftrightarrow 1.50$
B	S/L ratio	gr/L	5.0	200	$-1 \leftrightarrow 5.0$	$+1 \leftrightarrow 200$
C	pH		8.0	13.0	$-1 \leftrightarrow 8.0$	$+1 \leftrightarrow 13.0$
D	H_2O_2	%	0.0	1.0	$-1 \leftrightarrow 0.0$	$+1 \leftrightarrow 1.0$

The quadratic polynomial regression model (Equation (1)) was used to predict the response behavior while varying the four independent variables:

$$R = a_0 + \sum_{i=1}^{4} a_i Y_i + \sum_{i=1}^{4} a_{ii} Y_{ii}^2 + \sum_{i=1}^{3} \sum_{j=i+1}^{4} a_{ij} Y Y_j \tag{1}$$

where R represents the response, including copper recovery percentage and Cu concentration. The intercept, linear, quadratic, and interaction coefficients are denoted by a_0, a_i, a_{ii}, and a_{ij}, respectively. The four independent variables, namely glycine acid concentration, solid/liquid ratio, initial pH, and H_2O_2 dosage, are represented by Y_i and Y_j. After achieving the quadratic polynomial model, analysis of variance (ANOVA) was applied to validate the provided model. Due to the complicated relationship of parameters, their fluctuating behavior was studied and explained individually.

2.5. Analytical Procedure

Inductively coupled plasma (ICP PlasmaQuant 9100 Series, Endress+Hauser company, Swiss) was used for the analysis of the leached metals present in the leach liquor. The metal leaching rate was expressed as the dissolved percentage of metal, which was measured by the difference between the amount of the dissolved metal and its initial amount. The mineralogical phase analysis was carried out using an X-ray diffractometer (XRD, EQUINOX3000, Thermo scientific, Massachusetts, United States). An X-ray fluorescence spectrometer (XRF, PW2400, Malvern, United Kingdom) was used for the multi-element analysis.

3. Results and Discussion

3.1. The Leaching Behavior of Base Metals

The aim of optimizing the leaching step is to find a selective low temperature and low chemical consumption process for metals. If there are many metallic components in a solid matrix, the selectivity of a leaching system can be obtained by the chemical affinity of

the component for the reagent and kinetic considerations. Even though the first strategy is based on the differences in the affinity of a given reagent for the various components, the second strategy is based on the different component's dissolution rates. In this step, the samples were leached in diluted nitric acid to recover silver [29], and 98% of silver was leached. Silver is used on the surface of panels; the 0.5 M diluted nitric acid dissolved 98% of the silver and less than 5% of lead, copper, zinc, and tin. These metals are more active than silver, but because of the 15 min of leaching time and the 0.5 M nitric acid concentration, only very small amounts of these metals dissolved. There was silver on the semiconductor layer as small silver threads, along with a very low amount of lead and tin metals. So, the silver was quickly exposed to acid due to the layer structure.

Following the elimination of silver, Figure 2 shows the dissolution rate of metallic components from end-of-life solar panels by glycine acid. The conditions of the experiments were: T = 25 °C, [GLY] = 0.5 mol/L, and S/L ratio = 20 gr/L. As shown in Figure 2, the dissolution of In, Ga, Te, and Se was negligible in comparison with other metals. It can be predicted that glycine would dissolve copper easily, but the glycine also dissolved zinc and cadmium by up to 87% and 64% under given conditions. Clearly, glycine forms a soluble complex with copper, cadmium, lead, and zinc. However, the log K stability constant is different for these metals. As reported in the research, the log K of glycine complexes with Cu is 8.56 (at an ionic strength of 0), and this value is higher than the log K values for Cd, Zn, and Pb, which are 4.7, 5.38, and, 5.47, respectively [80,81].
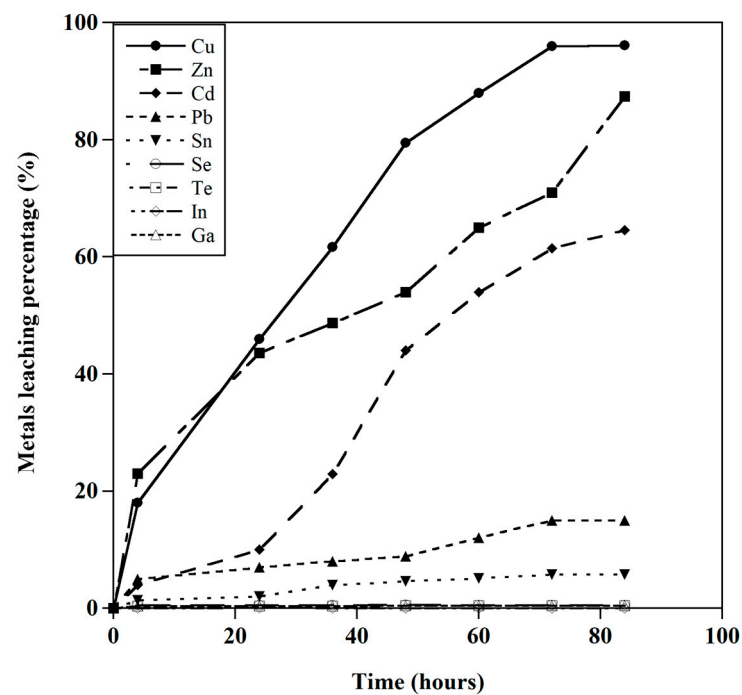

Figure 2. The leaching behavior for glycine concentration = 0.5 M, particle size ≤1 mm, T = 25 °C, S/L ratio = 20 gr/L.

As shown in Figure 2, the dissolution of zinc is faster and higher than that of cadmium. The standard reduction potentials of zinc, cadmium, and copper are −0.76 V, −0.4 V, and 0.34 V, respectively [82].

Regarding the different dissolution percentages of Zn and Cd, the probable reaction which can occur is cementation:
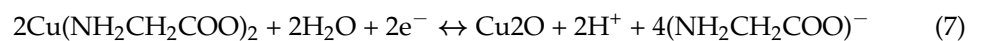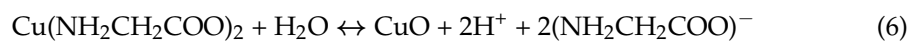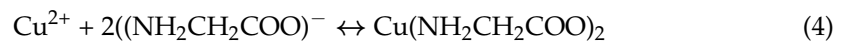
$$Cd^{2+} + Zn = Zn^{2+} + Cd. \tag{2}$$

It is probable for the dissolved Cd to be cemented by undissolved Zn, leading to a higher percentage of Zn dissolution compared with Cd, especially at the initial stages of

the leaching process. Due to the standard reduction potentials of metals, the cementation of cadmium occurred in the presence of low amounts of solid zinc [83,84].

　　When 50% of the zinc was dissolved, the dissolution of cadmium suddenly increased. In contrast, the dissolution of zinc and copper occurred simultaneously at the beginning of the leaching process, and after that, the dissolution of copper was much faster than that of zinc. As shown in Figure 2, glycine could not dissolve In, Ga, Se, and Te under these conditions, and the dissolution of tin was very low compared with other base metals.

3.1.1. Effect of Initial pH

　　According to reports [79,85,86], glycine forms soluble complexes with both cupric and cuprous ions and an equilibrium between copper oxides and copper glycinate as shown in the equations below:

$$Cu^{2+} + (NH_2CH_2COO)^- \leftrightarrow Cu(NH_2CH_2COO)^+ \tag{3}$$

$$Cu^{2+} + 2((NH_2CH_2COO)^- \leftrightarrow Cu(NH_2CH_2COO)_2 \tag{4}$$

$$Cu^+ + 2((NH2CH2COO)^- \leftrightarrow Cu(NH_2CH_2COO)^- \tag{5}$$

$$Cu(NH_2CH_2COO)_2 + H_2O \leftrightarrow CuO + 2H^+ + 2(NH_2CH_2COO)^- \tag{6}$$

$$2Cu(NH_2CH_2COO)_2 + 2H_2O + 2e^- \leftrightarrow Cu2O + 2H^+ + 4(NH_2CH_2COO)^- \tag{7}$$

　　There are different species of glycine in solution at different pH values, as shown in Table 3 [79,87]. The region of stability for the species in the Cu–glycine–water system is shown in Figure 3a. Increasing the initial pH to a certain level is expected to enhance the extraction efficiency of copper.

Table 3. Stability constants amounts of copper glycinate species at 25 °C and 1 atm [79].

Reaction	Stability Constant
$Cu^{2+} + 2(NH_2CH_2COO)^- = Cu(NH_2CH_2COO)_2$	15.64
$Cu^{2+} + (NH_2CH_2COO)^- = Cu(NH_2CH_2COO)^+$	8.57
$Cu^+ + 2(NH_2CH_2COO)^- = [Cu(NH_2CH_2COO)_2]^-$	10.1
$Cu(NH_2CH_2COO)^+ + H^+ = Cu(NH_3CH_2COO)^{2+}$	2.92
$(NH_2CH_2COO)^- + H^+ = Cu(NH_3CH_2COO)$	9.778
$H(NH_2CH_2COO) + H^+ = H_2(NH_2CH_2COO)^+$	2.350

　　Figure 3b illustrates the copper recovery at various initial pH values, a temperature of 25 °C, and a solid/liquid ratio of 20 gr/L. The experiments were conducted with a glycine acid concentration of 0.5 M. Glycine has been found to be an effective leaching agent for copper extraction from other sources, such as ore [88–90] and PCB waste [91–93], as reported in previous studies.
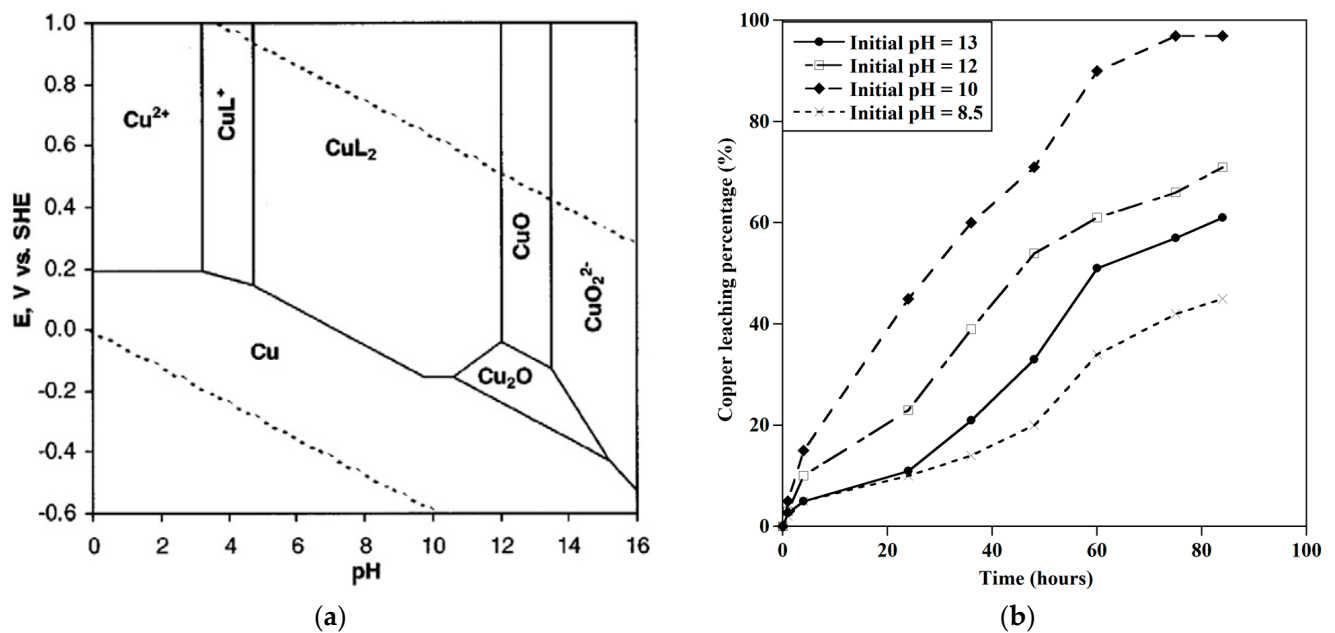
Figure 3. (**a**) Potential/pH diagram for the Cu–water–glycine system at 25 °C and 1 atm [79]. (**b**) Effect of initial pH on the extraction of Cu at glycine concentration = 0.5 M, S/L ratio = 20 gr/L, particle size = 1 mm, T = 25 °C.

In this step, experiments were conducted with pH values ranging from 8 to 13. As shown in Figure 3b, at a time of 60 h, increasing the pH from 8 to 10 led to a significant increase in copper extraction yield from 38% to 90%. However, this trend stopped at pH values above 10 due to the formation of insoluble Cu_2O or CuO, according to the Eh–pH diagram [93]. The leaching reaction for copper was controlled by stabilizing the formation of complexes with Cu ions and glycinate anions [93]. The optimized condition for the highest Cu extraction (96.9%) was found to be at pH 10 after 75 h, as shown in the Eh–pH diagram in Figure 3a.

The leaching behavior of other metals was investigated at the optimized conditions for copper extraction. Figure 4 shows that at an initial pH of 10 and a glycine concentration of 0.5 M, zinc extraction achieved about 88% recovery after 84 h, whereas lead extraction did not exceed 11.3%. It is expected that Zn^{2+} and Pb^{2+} form different complexes with glycinate anions, which may explain the differences in their extraction rates [94,95]. Although stable lead–glycinate complexes formed at initial pH values above 10, the dissolution rate of lead did not increase significantly. The main point of this step is the selective leaching of copper, zinc, and cadmium over other metals at a pH of 10. As shown in Figure 4, lead and tin can be dissolved completely by increasing the pH to 13. Based on the leaching behavior of the metals, it is recommended that the dissolution of copper and zinc be carried out at pH 10 in a countercurrent process. In contrast to the other metals, the leaching of cadmium decreased when the initial pH was increased, and its dissolution by glycine 0.5 M reached a maximum of 73% at pH levels below 10. In the second step, the leaching of lead and tin can be conducted in a countercurrent process at pH 13, achieving extraction rates of 62% and 81.8%, respectively.
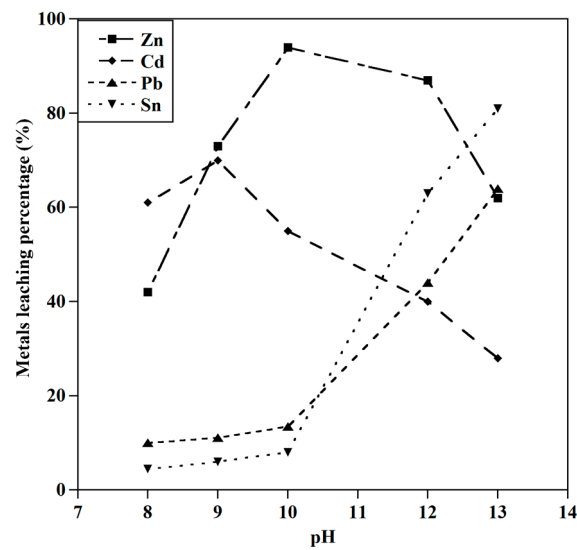
Figure 4. Effect of pH on the leaching behavior of metals. (Glycine concentration = 0.5 M, T = 25 °C, S/L ratio = 20 gr/L, particle size = 1 mm, t = 84 h).

3.1.2. Effect of Glycine Acid Concentration

Figure 5 illustrates the copper and lead recovery at various acid concentrations at a temperature of 25 °C and a solid/liquid ratio of 20 gr/L. Experiments were conducted over a range of acid concentrations from 0.1 M to 1.5 M to evaluate the effect of glycine concentration while keeping the initial pH, solid-to-liquid ratio, and temperature constant at pH 10, 20 gr/L, and 25 °C, respectively. Based on the glycine-to-copper molar ratio, an increase in acid concentration is expected to increase the extraction yield of copper. As shown in Figure 5, copper recovery was enhanced by increasing the acid concentration from 0.1 M to 1.5 M. However, above acid concentrations of 0.5 M, there was no significant increase in copper extraction. Moreover, above an acid concentration of 0.5 M, the extraction of copper and zinc was decreased. The effect of increasing the glycine acid concentration on zinc dissolution behavior is similar to that of copper leaching, and the optimized leaching of zinc is achieved at a 0.5 M glycine solution concentration. The leaching of other metals was investigated at different acid concentrations. Figure 5 shows that increasing the glycine concentration from 0.1 M to 1.5 M had a positive effect on the extraction of lead and cadmium.
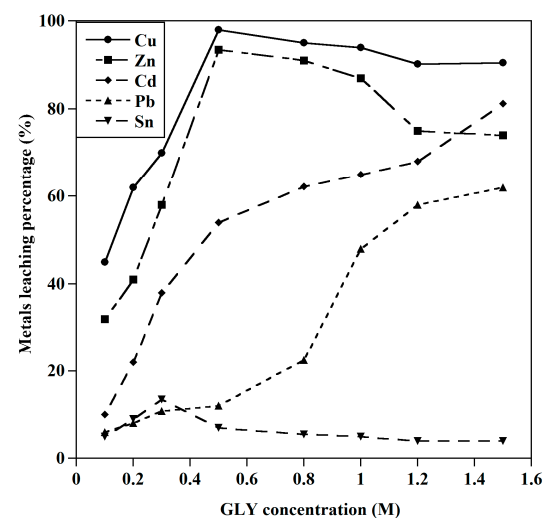

Figure 5. The effect of [GLY] concentration on the leaching behavior of metals (T = 25 °C, S/L ratio = 20 gr/L, initial pH = 10, t = 84 h).

3.1.3. Effect of the Solid/Liquid Ratio

The influence of the solid/liquid ratio on the recovery of copper and other base metals was investigated from 5 to 200 gr/L, and the optimized ratio controls the consumption of the leaching agent. The conditions of the experiments were kept at the initial pH of 10, an acid concentration of 0.5 M, and 25 °C. As shown in Figure 6, the dissolution of copper will increase when the S/L ratio decreases from 5 gr/L to 200 gr/L. However, there is no significant difference in the range of 5–20 gr/L. Similarly to copper extraction, this decreasing trend when the S/L ratio increases is seen in the extraction of other metals.
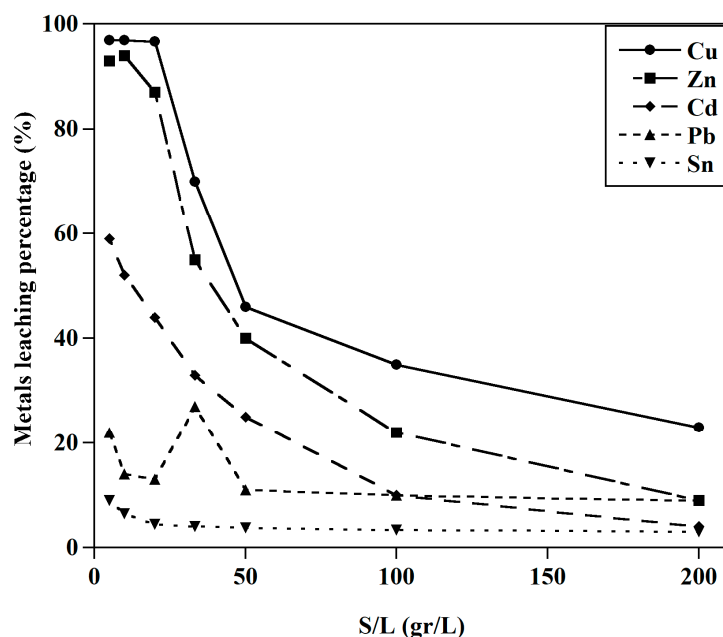
Figure 6. The effect of the S/L ratio on the leaching behavior of metals (T = 25 °C, [GLY] = 0.5 M, initial pH = 10, t = 84 h).

3.1.4. Effect of Temperature

To investigate the influence of temperature on the extraction of metals, experiments were conducted at an elevated 45 °C temperature at 0.5 M glycine, S/L ratio of 20 gr/L, and initial pH of 10. As shown in Figure 7, the extraction of copper and cadmium increased very little with the increase in temperature. But the results showed that the increasing of temperature reduced the extraction of lead, zinc, and tin. Due to the decomposition of glycine through deamination and decarboxylation, the pH of the solution can be reduced during the leaching process [86,96]. The decrease in zinc, lead, and tin extraction was due to the decrease in the solution pH. Also, the increase in cadmium extraction could be caused by this phenomenon.
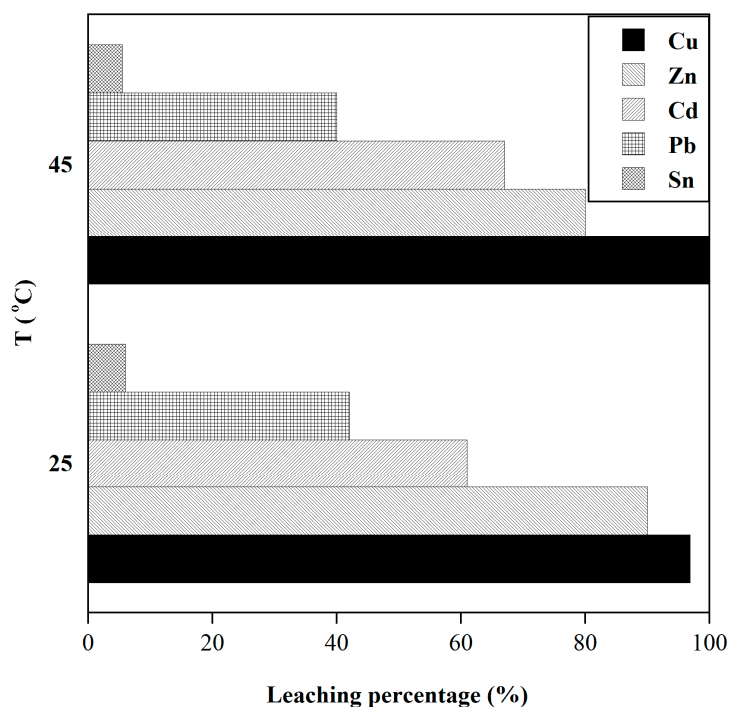
Figure 7. Effect of temperature on the extraction of metals ([GLY] = 0.5 M, S/L ratio = 20 gr/L, initial pH = 10, t = 84 h).
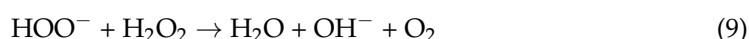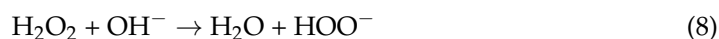
3.1.5. Effect of Hydrogen Peroxide

Hydrogen peroxide (H_2O_2) is used as an oxidizing agent in the leaching procedure, as the dissolution of metals with high reduction potentials is increased by applying a strong oxidant [97]. H_2O_2 is a strong oxidant with a standard electrode potential of 1.83 V, making it useful in the copper leaching system [98,99]. To evaluate the effect of oxidants on the extraction of base metals, experiments with H_2O_2 additions were conducted in comparison with ambient O_2. The experiments were carried out at a glycine concentration of 0.5 M, an initial pH of 10, a solid-to-liquid ratio of 5 gr/L, and at room temperature, using solid samples with a particle size of less than 1 mm. Figure 8 shows the extraction of copper over 84 h of leaching.

As expected, the application of H_2O_2 increased the dissolution of copper, particularly in the initial hours of leaching. At the 48 h mark, the addition of 0.5–1% H_2O_2 increased the copper extraction from 71% in ambient O_2 to 90% in the presence of 1% H_2O_2.

Figure 9 shows that the effects of an increasing H_2O_2 concentration on the extraction of other metals were different. Nonetheless, the dissolution of zinc, tin, lead, and cadmium was slightly improved by the addition of 1% H_2O_2.

Based on reports, at high pH values, the generation of hydroxide ions and oxygen occurs due to the decomposition of H_2O_2 as shown in the equations below:

$$H_2O_2 + OH^- \rightarrow H_2O + HOO^- \tag{8}$$

$$HOO^- + H_2O_2 \rightarrow H_2O + OH^- + O_2 \tag{9}$$

$$H_2O_2 \rightarrow 2OH^* \tag{10}$$

The generated hydrogen radical (OH^*) improved the leaching of cadmium and tin due to the high standard reduction potential. Also, the decomposition of H_2O_2 into O_2 generated an additional oxidant [100].
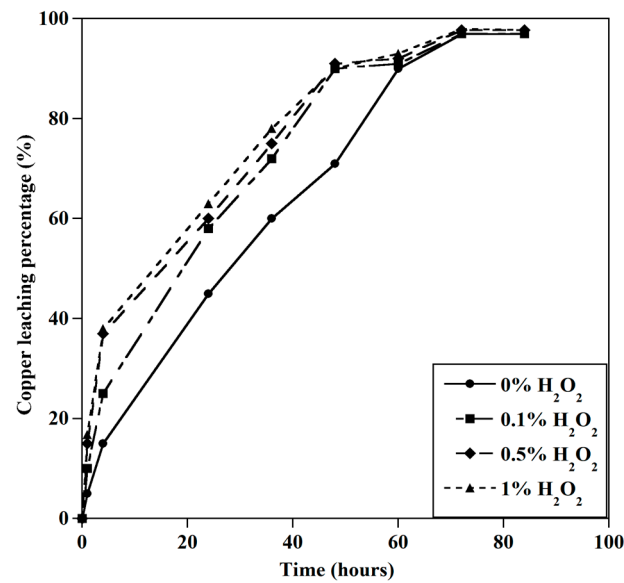
Figure 8. Effect of H_2O_2 on the leaching of copper (T = 25 °C, [GLY] = 0.5 M, S/L ratio = 5 gr/L, initial pH = 10, t = 84 h).
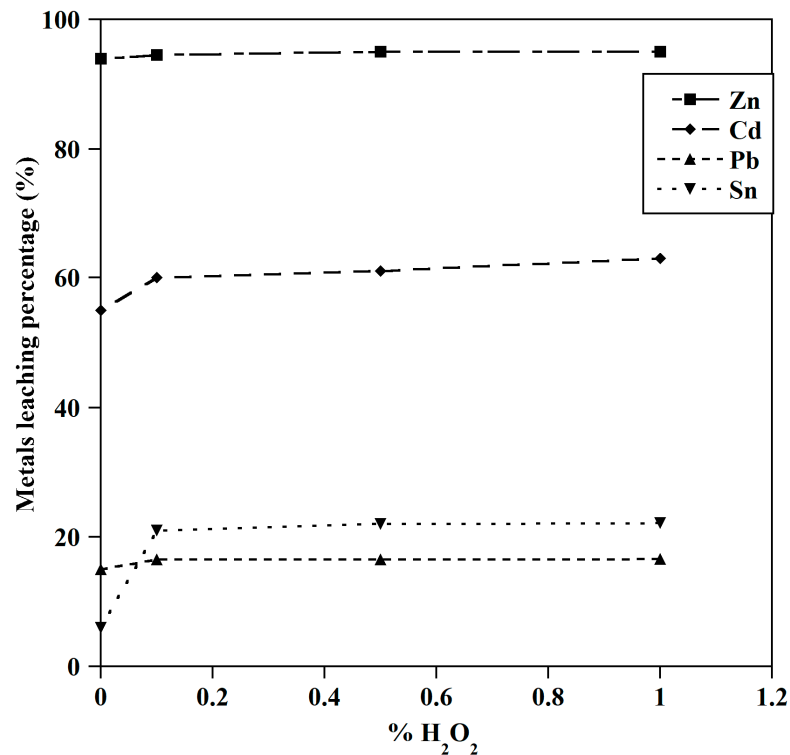
Figure 9. The effect of H_2O_2 on the leaching of metals (T = 25 °C, [GLY] = 0.5 M, S/L ratio = 5 gr/L, initial pH = 10, t = 84 h).

The insignificant change in lead dissolution with the increase in H_2O_2 dosage was due to a decrease in pH caused by the oxidation of glycine by H_2O_2 [86].

3.1.6. The Optimization of the Leaching Condition

The interaction of parameters indicates that the effect generated by changing one variable depends on the levels of other variables. The optimized conditions were calculated by analyzing the data for the leaching of copper, zinc, cadmium, lead, and tin. Based on the responses and the analysis of the variance presented in Table 4, a statistical model using the

Box–Behnken model was computed to determine the extraction of all metals. The coefficient of determination (R^2), adjusted R-square (adj. R^2), and analysis of variance (ANOVA) tests were employed to assess the adequacy of the proposed model and its goodness of fit. The goodness-of-fit statistics for all the response models are provided in Tables 5 and 6. As reported, the high values in the models were representative of the significant models. Also, as can be observed, the *p*-values of the models are negligible, which indicates that the proposed models had unity and significance. The determination coefficients were above 0.90 for all the metals, indicating the appropriate efficiency of the proposed models. The semi-empirical relation for copper-extraction-containing interactions between the existing parameters is defined in Table 5. The coefficients of these relations for the other metals are defined in the Supplementary Materials section. The positive terms indicate a synergistic effect on the extraction, whereas the negative terms express antagonism. As discussed in the prior section, the effect of the parameters was consistent with actual results.

Table 4. Response surface design of experiments.

Std. Run No.	Run	Factor 1 A:[GLY]	Factor 2 B: S/L	Factor 3 C: pH	Factor 4 D: H_2O_2	Response 1 Recovery of Copper	Response 2 Recovery of Zinc	Response 3 Recovery of Cadmium	Response 4 Recovery of Lead	Response 5 Recovery of Tin
		M	gr/L	%	%	%	%	%	%	%
9	1	0.1	100	10	1	25	20	4.8	1.5	2
16	2	1	20	10	0	92	88	62	44	5.5
20	3	1.5	100	10	0.5	36	22.8	31	51	2.4
2	4	1.5	20	10	0	90	72.5	81	67	5.6
14	5	1	10	10	0	92	88.5	75	57	5
7	6	0.8	100	10	0	28	17	25	15	4.1
15	7	0.8	50	10	0.5	54.6	49.1	37.5	21.5	9.1
4	8	1.5	10	13	0	62	55	72	97.8	98
26	9	1.5	5	9	1	43	55	99	60	5
10	10	1.5	5	10	1	93	75	84	62	6
1	11	0.1	5	10	0	40	30	10	5	5
3	12	0.1	200	10	0.5	12	11	0	0	0
22	13	1.5	5	13	1	65	56	73	99.8	99.7
8	14	0.8	100	13	0	14	11	20	77	54
19	15	0.1	100	13	0.5	21	18	0	16	24
18	16	1.5	100	8	0.5	18	11.5	27	14	7.4
25	17	0.5	100	10	0.5	43	34	17	7	3
27	18	0.8	100	10	0.5	33	25	29.5	15	2
12	19	0.5	20	10	1	98.5	98.1	62	16	5.8
28	20	0.8	100	10	0	28	17	31.7	22	4.1
17	21	0.1	100	8	0.5	16	15	3.2	1	2
23	22	0.8	20	10	1	72	69	29.9	24	10.3
6	23	0.5	20	13	0	67	62	19.5	81.9	64.9
5	24	0.8	50	10	0.5	54.6	49.1	19.5	21.5	9.1
24	25	0.8	200	10	1	36	28	13	21	8
11	26	0.1	100	10	1	22.5	18.1	7.8	7	7
13	27	0.5	10	10	0.5	99	99	60	22	10
21	28	0.5	10	10	1	99.9	99.5	63	22.1	11

Table 5. ANOVA table of copper recovery for the Quadratic and Reduced Quadratic models.

Analyzed Model	Quadratic Model				Reduced Quadratic Model			
Recovery of Copper								
	Coefficient	Sum of Squares	F-Value	*p*-Value	Coefficient	Sum of Squares	F-Value	*p*-Value
Intercept	38.64				98.167			
[GLY]	3.99	78.68	0.40	0.5404	92.94	109.83	0.64	0.4346
S/L	−31.18	3101.11	15.58	0.0017	−0.948	6072.01	35.23	<0.0001
pH	−0.45	0.51	0.00	0.9606	−4.8370	36.40	0.21	0.6510
H_2O_2	1.27	7.70	0.04	0.8471	−40.319	210.62	1.22	0.2828
[GLY] * S/L	3.85	29.53	0.15	0.7064				
[GLY] * pH	−7.75	178.75	0.90	0.3606				
[GLY] * H_2O_2	−20.29	1826.81	9.18	0.0097	−46.35	2240.58	13.00	0.0019
S/L * pH	−7.61	42.40	0.21	0.6521				
S/L * H_2O_2	−4.01	40.75	0.20	0.6584				
pH * H_2O_2	8.70	235.23	1.18	0.2968	8.15275	407.07	2.36	0.1408
$[GLY]^2$	−17.66	1056.01	5.31	0.0384	−40.279	2432.72	14.12	0.0013
S/L^2	35.90	2183.67	10.97	0.0056	0.003	3282.95	19.05	0.0003
pH^2	−7.81	104.79	0.53	0.4810				
$H_2O_2{}^2$	−8.74	322.93	1.62	0.2251				
Model summary		21,697.64	7.79	0.0003		21,010.85	15.24	<0.0001
		Significant				**Significant**		
Residual Lack of Fit		2587.76	-	-		3274.55	-	-
		Not Significant *				**Not Significant ***		

* Based on analysis of the Externally Studentized Residuals vs. Normal % Probability graphs.

Table 6. Fit statistics for the suggested models.

	Model	R^2	Adjusted R^2	Predicted R^2	ANOVA *p*-Value
Recovery of Copper	Quadratic model	0.893	0.779	−0.674	0.0003
	Reduced Quadratic model	0.865	0.808	0.576	<0.0001
Recovery of Zinc	Quadratic model	0.928	0.851	−0.040	<0.0001
	Reduced Quadratic model	0.909	0.878	0.811	<0.0001
Recovery of Cadmium	Quadratic model	0.920	0.834	0.316	<0.0001
	Reduced Quadratic model	0.902	0.860	0.800	<0.0001
Recovery of Lead	2FI model	0.926	0.883	0.313	<0.0001
	Reduced 2FI model	0.906	0.879	0.670	<0.0001
Recovery of Tin	Quadratic model	0.980	0.958	0.632	<0.0001
	Reduced Quadratic model	0.967	0.958	0.831	<0.0001

Note: R^2 represents the coefficient of determination; adjusted R^2 represents the adjusted coefficient of determination; Predicted R^2 represents the predicted coefficient of determination; and ANOVA *p*-value indicates the statistical significance of the model fit.

As shown in Figure 10, the leaching condition for copper was plotted by the Minitab software Version 21.1.0: [GLY] = 0.5 M, S/L ratio = 10 gr/L, pH = 10, and H_2O_2 = 1%. Similarly to copper, based on the results of the experiments, the optimal leaching conditions for other metals are reported in Table 7.

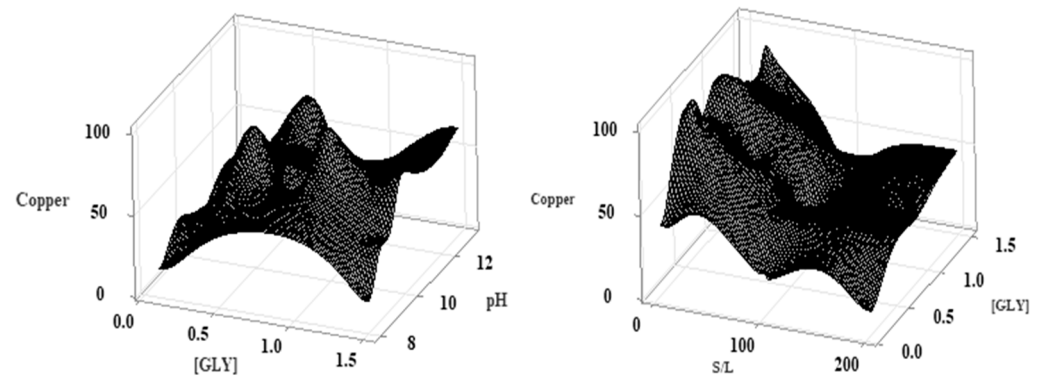**Figure 10.** The RSM plot of Cu recovery.

Table 7. The optimal conditions for the leaching of metals.

	[GLY] (M)	S/L (gr/L)	pH	H_2O_2 (%)	Recovery (%)
Copper	0.5	10	10	1	99.9
Zinc	0.5	10	10	1	99.5
Cadmium	1.5	5	9	1	99
Lead	1.5	5	13	1	99.8
Tin	1.5	5	13	1	99.7

3.2. The Leaching Behavior of Valuable Metals

The residue from the base metal leaching process was washed with double-distilled water, filtered, and then utilized as the raw material for the leaching of other metals. The residue from the base metal leaching was roasted at a constant temperature of 400 °C for a specified time to achieve phase transformation. Previous studies have identified the first exothermic peak in the DTA curve at 370 °C for the oxidation of CIGS at the surface [101,102]. Additionally, the temperature range of 200–400 °C has been determined to produce In_2O_3 and Ga_2O_3 [103]. Therefore, a temperature of 400 °C was selected for roasting for a duration of 1 h. Figure 11 illustrates the XRD pattern of the dried and roasted leaching residue after glycine leaching. As predicted, the formation of SeO_2, Ga_2O_3, and In_2O_3 was achieved due to thermal oxidation. The presence of $CuIn_{0.5}Ga_{0.5}Se_2$ and SnO_2 in the pattern indicates the existence of a low amount of copper and tin in the sample. The reason is that the glycine leaching experiments before roasting were conducted at an S/L ratio of 20 gr/L. Table 8 shows the content of the dried material analyzed after the glycine leaching step. Due to the nature of the existing phases, it appears that indium and gallium form soluble species in the lower pH range. According to the Hard–Soft Acid Base (HSAB) concept, strong acids such as In^{3+} and Ga^{3+} prefer to bind to strong bases such as Cl^- to form ionic complexes. Therefore, it is expected that HCl would be a suitable leaching agent for the dissolution of indium and gallium [104–106].

Table 8. The XRF results of the major metal contents of the glycine leaching residue (feed material for HCl leaching).

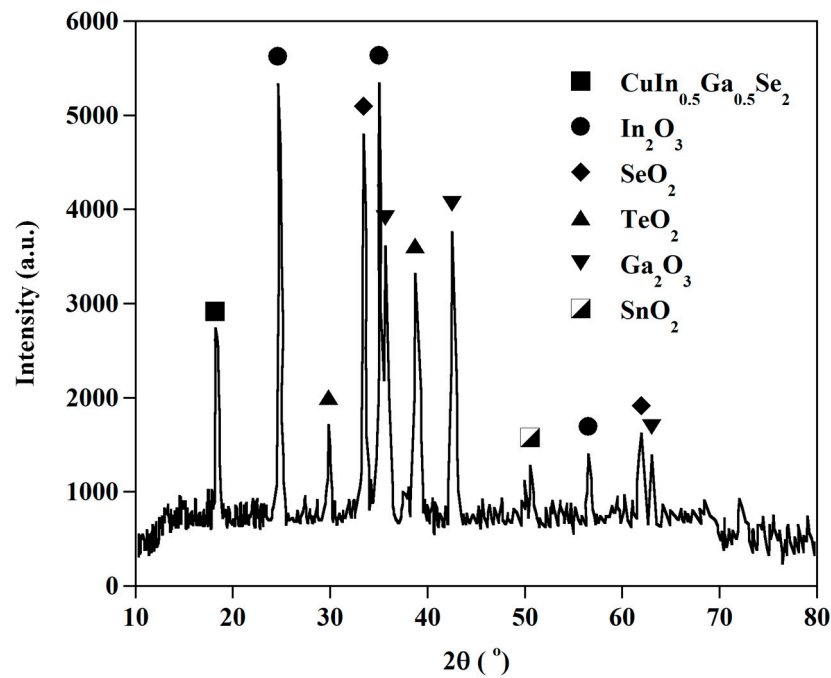|	Cu	Pb	Sn	Se	In	Ga	Te
Metal content (Wt.%)	5	1.1	3.9	23.2	10.4	9.8	25

Figure 11. XRD pattern of glycine leaching residue after oxidation roasting.

Figure 12 illustrates the recovery of In, Ga, Se, and Te under the following leaching conditions: [HCl]: 4 M, T = 25 °C, S/L ratio = 10 gr/L. As shown in Figure 13, the leaching efficiencies for gallium and indium increased as a function of time. As predicted, the recovery of indium and gallium was 93% and 71%, respectively, and became saturated at 100 min. Selenium and tellurium were recovered at 21.8% and 11.5%, respectively, as shown in Figure 13. However, a significant amount of tellurium and selenium was not dissolved, which could be due to the lack of soluble species of selenium and tellurium at this range of concentrations.
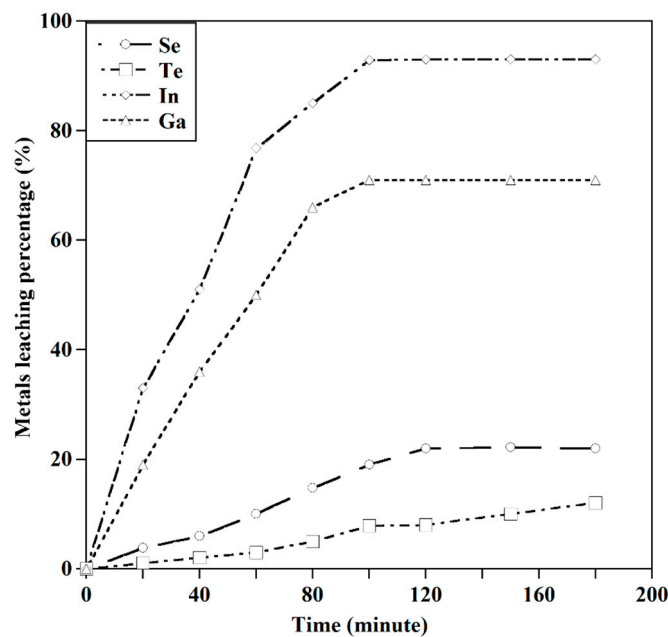

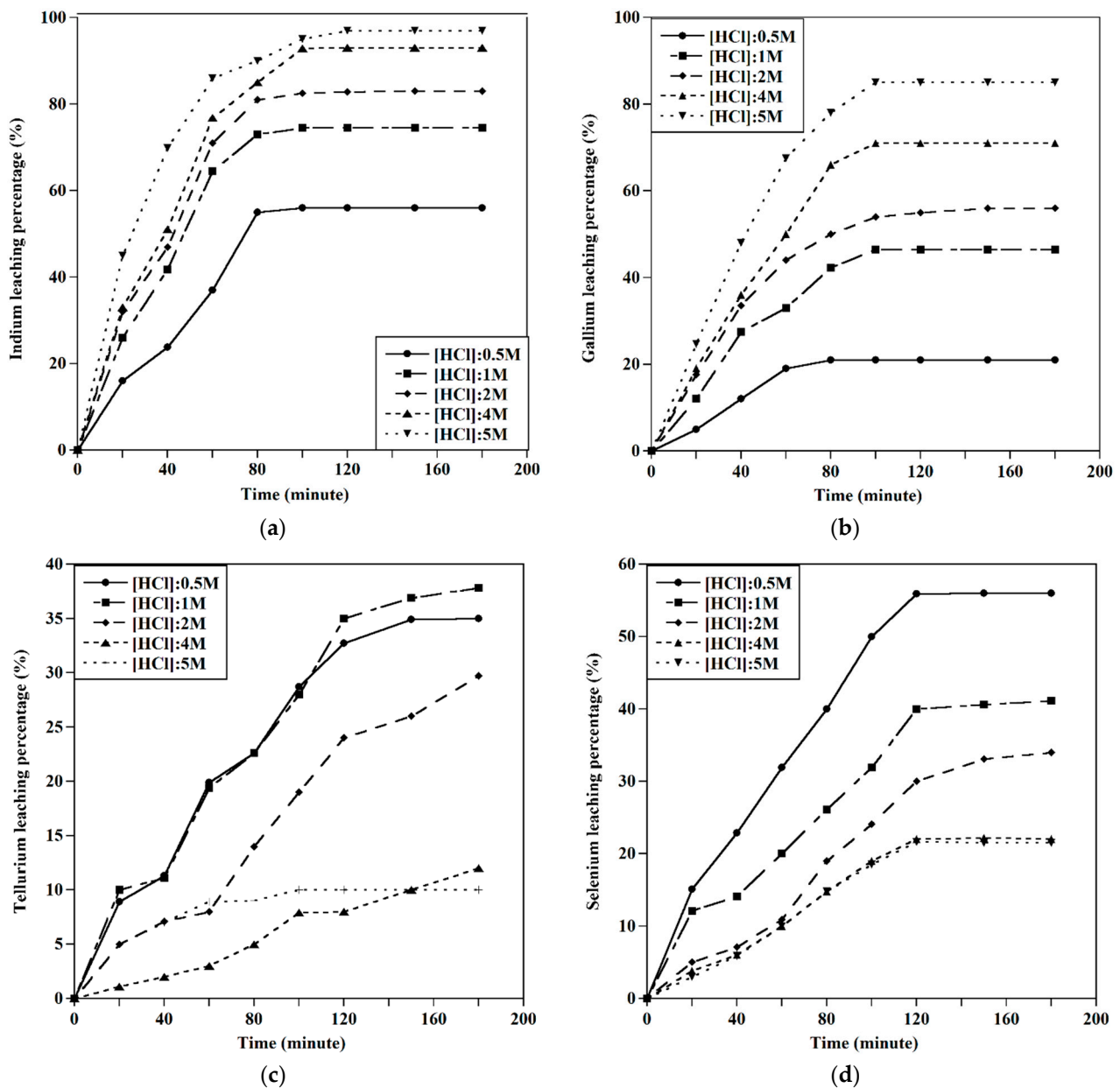**Figure 12.** The leaching behavior of In, Ga, Se, and Te ([HCL] = 4 M, T = 25 °C, S/L ratio = 10 gr/L).

Figure 13. The effect of HCl concentration on the leaching behavior of metals (T = 25 °C, S/L ratio = 10 gr/L). (**a**) Leaching of indium. (**b**) Leaching of gallium. (**c**) Leaching of tellurium. (**d**) Leaching of selenium.

3.2.1. Effect of HCl Concentration

The effect of HCl concentration on the leaching efficiency of the sample was investigated with acid concentrations ranging from 0.5 M to 4 M. As shown in Figure 13a,b, the recovery of indium and gallium increased with increasing acid concentration. When the acid concentration increased from 0.5 M to 5 M, the leaching efficiency of indium and gallium increased from 56% to 97% and from 21% to 85%, respectively. However, as shown in Figure 13d, the leaching of selenium decreased with an increase in acid concentration. This issue could be related to the range of stability of Se species. Soluble species, including H_2SeO_3 and $HSeO_4$, exist at acidic pH values [107]. However, at decreasing pH values, selenium precipitates as elemental Se. Thus, increasing the acid concentration promotes the precipitation of selenium and decreases its leaching efficiency.

The leaching percentage of selenium increased from 21.8% to 56.7% when the acid concentration was reduced from 5 M to 0.5 M. However, the effect of acid concentration

effect on tellurium recovery was more complicated. Te^{4+} exists in the form of ions such as $Te(OH)_3^+$ or $TeO(OH)^+$ at very low pH ranges. As seen in Figure 13c, the highest recovery percentage of tellurium (37.5%) was obtained at an acid concentration of 1 M. This could be due to the narrow region of soluble $Te(OH)_3^+$ species at low pH values [108], which results in a low leaching rate of tellurium under these conditions.

3.2.2. Effect of the S/L Ratio

The effect of the solid/liquid ratio from 5 to 200 gr/L on indium, gallium, selenium, and tellurium recovery was investigated. The conditions of the experiments were kept at an acid concentration of 5 M and a temperature of 25 °C. As shown in Figure 14, the dissolution of copper will increase when the S/L ratio decreases from 5 gr/L to 200 gr/L. As predicted, a decreasing trend is seen in the extraction of other metals when the S/L ratio increases.
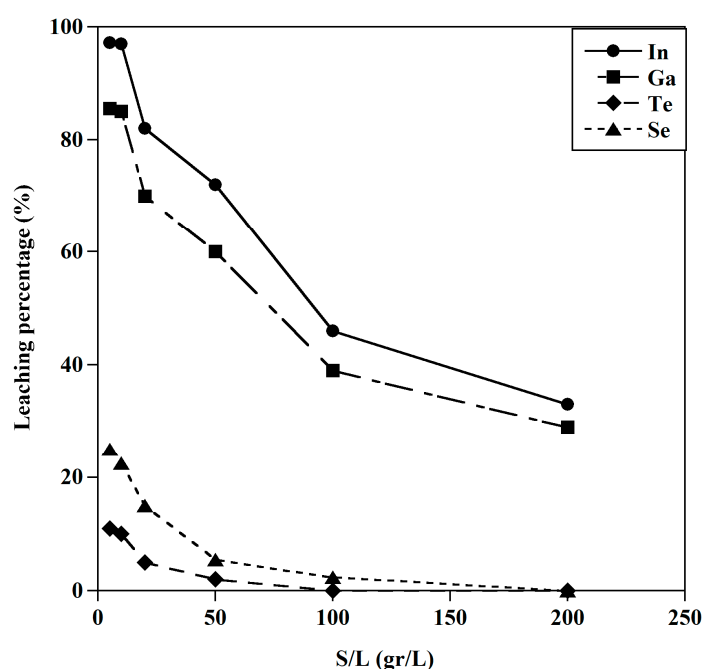

Figure 14. The effect of the S/L ratio on the leaching behavior of metals (T = 25 °C, [HCl] = 5 M, t = 120 min).

3.2.3. Effect of Temperature

The effect of temperature on the extraction of metals was studied in the range of 25–60 °C. Based on the optimal conditions for the In, Ga, Se, and Te recovery, two different conditions were considered. As shown in Figure 15a, the HCl concentration was 5 M for the high-level extraction of indium and gallium in the temperature range of 25–45 °C. The results indicated that increasing the temperature improved the extraction of indium and gallium to about 100%. Considering the second condition at the [HCl] of 0.5 M, the extraction of selenium was increased by increasing of temperature to 60 °C. On the contrary, the increasing the temperature reduced the extraction of tellurium. This can be caused due to the narrow range of tellurium species at elevated temperatures. This decreasing trend in tellurium extraction by the increase in temperature was seen for the sulfuric acid solution [109]. As shown in Figure 15b, the increasing temperature has a positive influence on the indium and gallium extraction at different acid concentrations. Selenium was recovered at about 100% at a temperature of 60 °C, whereas tellurium extraction at this temperature was achieved at less than 10%.
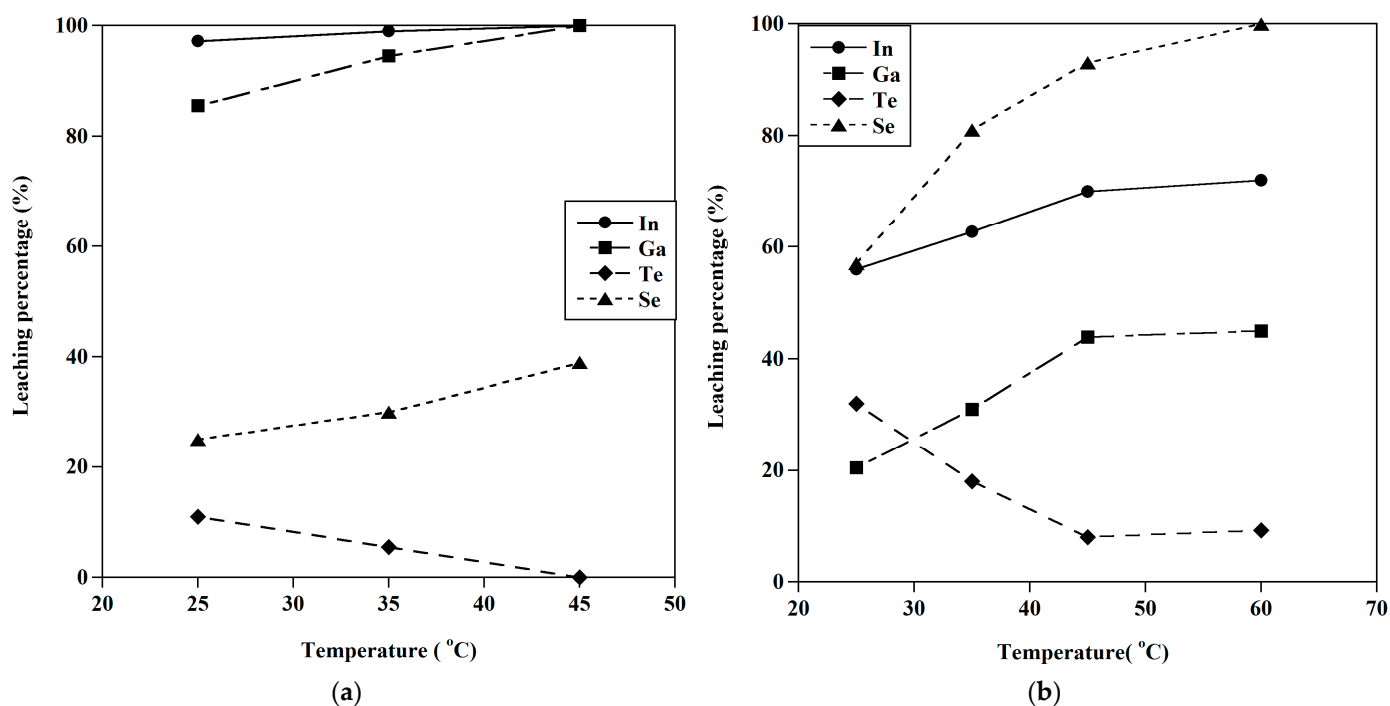
Figure 15. The effect of temperature on the metal extraction. (**a**) [HCl] = 5 M, S/L ratio = 10 gr/L; t = 120 min (**b**) [HCl] = 0.5 M, S/L ratio = 10 gr/L, t = 120 min.

4. Suggested Flowsheet for Recycling All Types of Solar Panels

Figure 16 represents an innovative and general flowsheet for the recycling of metals from all types of solar panels. The separation of the metallic and non-metallic parts was confirmed by the physical separation, shredding, and thermal treatment. As discussed, the silver extraction was conducted by diluted nitric acid in the first leaching step. Based on this figure, the glycinate solution was used for the leaching of copper, zinc, and cadmium in one step, and other metals such as lead, tin, and the cadmium residue were dissolved by a 1.5 M glycine solution in the second step. The raffinate, which includes zinc, cadmium, and copper, is processed in our research by a solvent extraction method. Additionally, the extraction of other metals such as lead, tin, and cadmium reached their optimized condition by changing various factors. The recovery of indium, gallium, tellurium, and selenium was examined under different conditions, and HCl was used as the leaching agent for the dissolution of indium and gallium. An interesting point was that the separation of tellurium and selenium was achieved by 0.5 M HCl at a temperature of 60 °C and a time of 120 min. Also, about 100% of indium and gallium were recovered by 5 M HCl at a temperature of 45 °C.
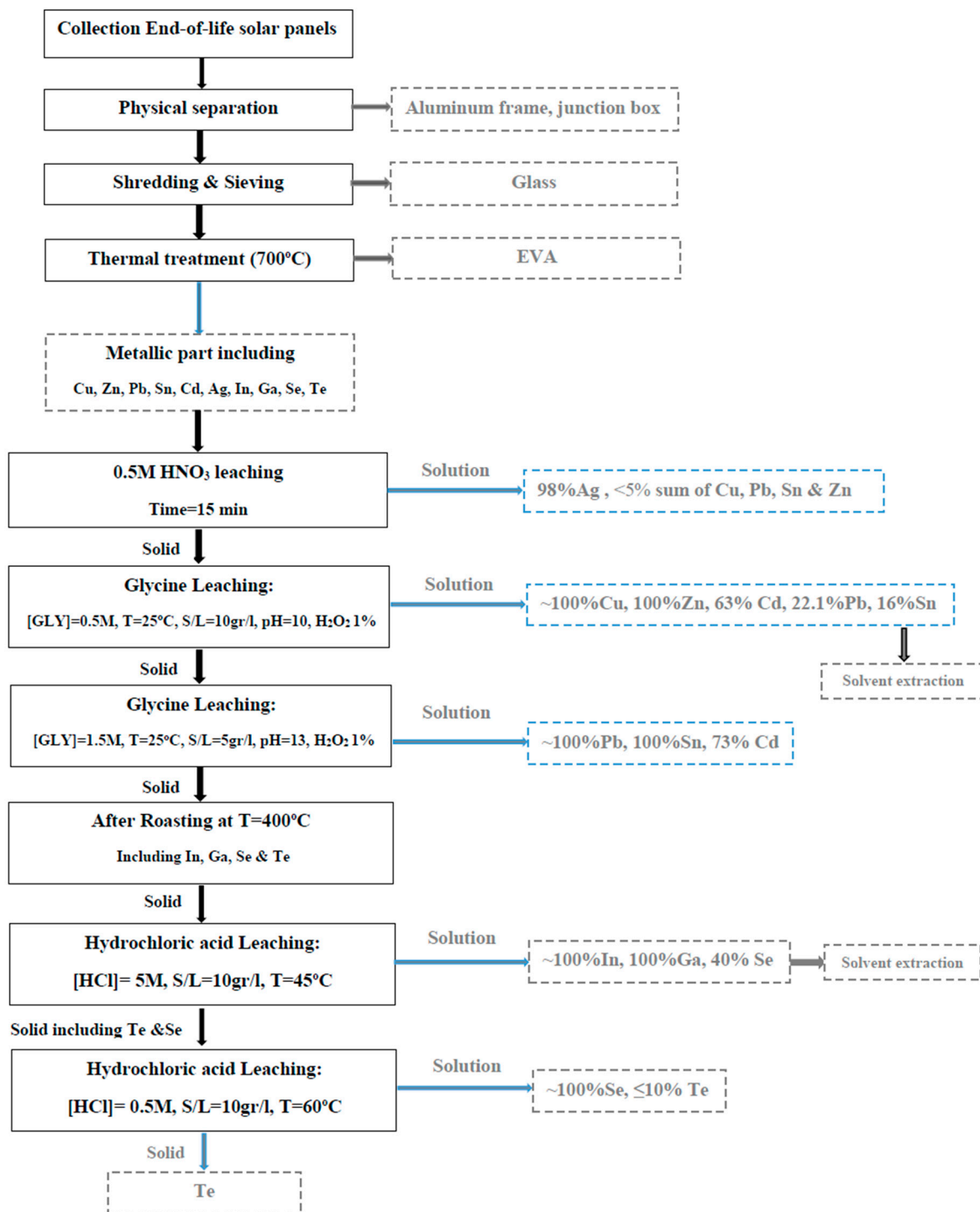
Figure 16. The general flowsheet for recycling all types of solar panels.

5. Conclusions

If the environmental effects of solar panel technology are to be evaluated according to the life cycle assessment, then the entire production process up to the time of retirement should be considered. To ensure the effectiveness of solar PV technology, it is necessary to consider all the environmental consequences of the significant growth of solar PV production. Comprehensive methods should be developed to recycle spent solar panels after their end of life to protect the environment and to achieve economic added value. Advanced research has been initiated to recover metals from various types of solar panels,

and this paper focuses on the leaching of base metals, which is the initial step of future research in this field.

This study presents an innovative approach for extracting metals (Cu, Ag, Cd, Te, Se, In, Ga, Sn, Pb, Zn) from all kinds of solar panels. The base metal extraction was a prerequisite for recovering precious metals from end-of-life solar panels. The initial step after preparation was the dissolution of silver using a 0.5 M HNO_3 solution. The leaching behavior of copper and other metals in an alkaline glycine solution was then studied under various conditions. The optimal conditions for the selective extraction of copper and zinc were found to be a glycine concentration of 0.5 M, an S/L ratio of 10 gr/L, and an initial pH value of 10. To achieve the highest extraction of other metals (Cd, Sn, Pb), the leaching procedure was performed at different initial pHs, and the optimized conditions for the extraction of Cu, Pb, Cd, Zn, and Sn were studied.

In the final step, the dissolution of indium, gallium, selenium, and tellurium was studied using HCl acid under different conditions. Indium and gallium were recovered under experimental conditions of [HCl] = 5 M, T = 45 °C, and S/L ratio = 10 gr/L, achieving recoveries of about 100%. By decreasing the acid concentration to 0.5 M, the extraction of selenium was achieved at about 100% at a temperature of 60 °C, and the complete separation of tellurium and selenium occurred.

This study demonstrates an innovative approach for extracting metals from all types of solar panels. A comprehensive method for recycling spent solar panels must be developed to ensure the effectiveness of solar PV technology and to reduce its environmental impact. The research on recovering metals from different types of solar panels is ongoing, and this paper presents the leaching step of metals, paving the way for future research in this field. Our hope is that, by conducting kinetic studies, the timing of experiments can be optimized. Also, by controlling the pH and temperature during the glycine leaching process, we can improve the efficiency of the leaching process. The solvent extraction method can separate copper, zinc, and cadmium from the glycine solution and indium and gallium from the final solution.

Supplementary Materials: The following supporting information can be downloaded at: https://www.mdpi.com/article/10.3390/met13101677/s1.

Author Contributions: M.K.—investigation, methodology, chemicals, formal analysis and data curation, funding acquisition, and writing the original draft; E.K.A.—supervision, conceptualization, methodology, data curation, review, and editing. All authors have read and agreed to the published version of the manuscript.

Data Availability Statement: Restrictions apply to the availability of these data. Data were obtained from Amirkabir University of Technology and are available from Eskandar Keshavarz Alamdari with the permission of Amirkabir University of technology.

Conflicts of Interest: The authors declare no conflict of interest.

References

1. Chowdhury, M.S.; Kazi, S.R.; Chowdhury, T.; Nuthammachot, N.; Techato, K.; Akhtaruzzaman, M.; Kiong Tiong, S.; Kamaruzzaman, S.; and Nowshad, A. An overview of solar photovoltaic panels' end-of-life material recycling. *Energy Strategy Rev.* **2020**, *27*, 100431. [CrossRef]
2. Briese, E.; Piezer, K.; Celik, I.; Apul, D. Ecological network analysis of solar photovoltaic power generation systems. *J. Clean. Prod.* **2019**, *223*, 368–378. [CrossRef]
3. Hosseinpour, A.; Tafaghodi Khajavi, L. Slag refining of silicon and silicon alloys: A review. *Miner. Process. Extr. Metall. Rev.* **2018**, *39*, 308–318. [CrossRef]
4. Nguyen, T.H.; Lee, M.S. A review on germanium resources and its extraction by hydrometallurgical method. *Miner. Process. Extr. Metall. Rev.* **2021**, *42*, 406–426. [CrossRef]
5. Irena, I.-P. End-of-life management: Solar photovoltaic panels. *Int. Renew. Energy Agency Int. Energy Agency Photovolt. Power Syst.* **2016**.

6. Fiandra, V.; Sannino, L.; Andreozzi, C.; Graditi, G. End-of-life of silicon PV panels: A sustainable materials recovery process. *Waste Manag.* **2019**, *84*, 91–101. [CrossRef]

7. Yi, Y.K.; Kim, H.S.; Tran, T.; Hong, S.K.; Kim, M.J. Recovering valuable metals from recycled photovoltaic modules. *J. Air Waste Manag. Assoc.* **2014**, *64*, 797–807. [CrossRef]

8. Xu, Y.; Li, J.; Tan, Q.; Peters, A.L.; Yang, C. Waste Management. 2018, 75, 450–458. *Int. J. Integr. Waste Manag. Sci. Technol.* **2018**, *75*, 450–458.

9. Cucchiella, F.; Rosa, P. End-of-Life of used photovoltaic modules: A financial analysis. *Renew. Sustain. Energy Rev.* **2015**, *47*, 552–561. [CrossRef]

10. Monier, V.; Hestin, M. Study on photovoltaic panels supplementing the impact assessment for a recast of the WEEE directive. *Final. Rep.* **2011**, *6*.

11. Evans, A.; Strezov, V.; Evans, T.J. Assessment of sustainability indicators for renewable energy technologies. *Renew. Sustain. Energy Rev.* **2009**, *13*, 1082–1088. [CrossRef]

12. Bhat, I.; Prakash, R. LCA of renewable energy for electricity generation systems—A review. *Renew. Sustain. Energy Rev.* **2009**, *13*, 1067–1073.

13. De Wild-Scholten, M. Energierücklaufzeiten für PV-module und systeme energy payback times of PV modules and systems. *Workshop Photovoltaik-Modul.* **2009**, *26*, 27.

14. Nain, P.; Kumar, A. Understanding manufacturers' and consumers' perspectives towards end-of-life solar photovoltaic waste management and recycling. *Environ. Dev. Sustain.* **2023**, *25*, 2264–2284. [CrossRef]

15. Bakhiyi, B.; Labrèche, F.; Zayed, J. The photovoltaic industry on the path to a sustainable future—Environmental and occupational health issues. *Environ. Int.* **2014**, *73*, 224–234. [CrossRef]

16. Płaczek-Popko, E. Top PV market solar cells 2016. *Opto-Electron. Rev.* **2017**, *25*, 55–64. [CrossRef]

17. Duda, J.; Kusa, R.; Pietruszko, S.; Smol, M.; Suder, M.; Teneta, J.; Wójtowicz, T.; Żdanowicz, T. Development of roadmap for photovoltaic solar technologies and market in Poland. *Energies* **2022**, *15*, 174. [CrossRef]

18. Li, X.; Liu, H.; You, J.; Diao, H.; Zhao, L.; Wang, W. Back EVA recycling from c-Si photovoltaic module without damaging solar cell via laser irradiation followed by mechanical peeling. *Waste Manag.* **2022**, *137*, 312–318. [CrossRef]

19. Vargas, C.; Chesney, M. End of life decommissioning and recycling of solar panels in the United States. A real options analysis. *J. Sustain. Financ. Investig.* **2021**, *11*, 82–102. [CrossRef]

20. Khawaja, M.K.; Ghaith, M.; Alkhalidi, A. Public-private partnership versus extended producer responsibility for end-of-life of photovoltaic modules management policy. *Sol. Energy* **2021**, *222*, 193–201. [CrossRef]

21. Palaniappan, S.K.; Chinnasamy, M.; Rathanasamy, R.; Kumar, S. Pal. "Recycling of Solar Panels. Recycling of Solar Panels. *Mater. Sol. Energy Convers. Mater. Methods Appl.* **2021**, 47–86. [CrossRef]

22. Pagnanelli, F.; Moscardini, E.; Abo Atia, T.; Toro, L. Photovoltaic panel recycling: From type-selective processes to flexible apparatus for simultaneous treatment of different types. *Miner. Process. Extr. Metall.* **2016**, *125*, 221–227. [CrossRef]

23. Abdo, D.M.; Mangialardi, T.; Medici, F.; Piga, L. D-Limonene as a Promising Green Solvent for the Detachment of End-of-Life Photovoltaic Solar Panels under Sonication. *Processes* **2023**, *11*, 1848. [CrossRef]

24. Azeumo, M.F.; Germana, C.; Ippolito, N.M.; Medici, F.; Piga, L.; Santilli, S. Photovoltaic module recycling, a physical and a chemical recovery process. *Sol. Energy Mater. Sol. Cells* **2019**, *193*, 314–319. [CrossRef]

25. Ganesan, K.; Valderrama, C. Anticipatory life cycle analysis framework for sustainable management of end-of-life crystalline silicon photovoltaic panels. *Energy* **2022**, *245*, 123207. [CrossRef]

26. Latunussa, C.; Ardente, F.; Blengini, G.A.; Mancini, L. Life Cycle Assessment of an innovative recycling process for crystalline silicon photovoltaic panels. *Sol. Energy Mater. Sol. Cells* **2016**, *156*, 101–111. [CrossRef]

27. Klugmann-Radziemska, E. Current trends in recycling of photovoltaic solar cells and modules waste/Recykling zużytych ogniw i modułów fotowoltaicznych-stan obecny. *Chem.-Didact.-Ecol.-Metrol.* **2012**, *17*, 89–95. [CrossRef]

28. Dias, P.; Javimczik, S.; Benevit, M.; Veit, H. Recycling WEEE: Polymer characterization and pyrolysis study for waste of crystalline silicon photovoltaic modules. *Waste Manage.* **2017**, *60*, 716–722. [CrossRef] [PubMed]

29. Dias, P.; Javimczik, S.; Benevit, M.; Veit, H.; Moura Bernardes, A. Recycling WEEE: Extraction and concentration of silver from waste crystalline silicon photovoltaic modules. *Waste Manage.* **2016**, *57*, 220–225. [CrossRef]

30. Savvilotidou, V.; Antoniou, A.; Gidarakos, E. Toxicity assessment and feasible recycling process for amorphous silicon and CIS waste photovoltaic panels. *Waste Manag.* **2017**, *59*, 394–402. [CrossRef]

31. Dias, P.; Schmidt, L.; Bonan Gomes, L.; Bettanin, A.; Veit, H.; Moura Bernardes, A. Recycling waste crystalline silicon photovoltaic modules by electrostatic separation. *J. Sustain. Metall.* **2018**, *4*, 176–186. [CrossRef]

32. Fthenakis, V.M.; Wang, W. Extraction and separation of Cd and Te from cadmium telluride photovoltaic manufacturing scrap. *Prog. Photovolt. Res. Appl.* **2006**, *14*, 363–371. [CrossRef]

33. Nekouaslazadeh, A. *Recycling Waste Solar Panels (c-Si & CdTe) in Sweden*; Digitala Vetenskapliga Arkivet: Borås, Sweden, 2021.

34. Kuczyńska-Łażewska, A.; Klugmann-Radziemska, E.; Witkowska, A. Recovery of Valuable Materials and Methods for Their Management When Recycling Thin-Film CdTe Photovoltaic Modules. *Materials* **2021**, *14*, 7836. [CrossRef] [PubMed]

35. Theocharis, M.; Tsakiridis, P.E.; Kousi, P.; Hatzikioseyian, A.; Zarkadas, I.; Remoundaki, E.; Lyberatos, G. Hydrometallurgical Treatment for the Extraction and Separation of Indium and Gallium from End-of-Life CIGS Photovoltaic Panels. *Mater. Proc.* **2021**, *5*, 51.

36. Gu, S.; Fu, B.; Dodbiba, G.; Fujita, T.; Fang, B. Promising approach for recycling of spent CIGS targets by combining electrochemical techniques with dehydration and distillation. *ACS Sustain. Chem. Eng.* **2018**, *6*, 6950–6956. [CrossRef]

37. Tao, M.; Fthenakis, V.; Ebin, B.; Steenari, B.M.; Butler, E.; Sinha, P.; Corkish, R.; Wambach, K.; Simon, E.S. Major challenges and opportunities in silicon solar module recycling. *Prog. Photovolt. Res. Appl.* **2020**, *28*, 1077–1088. [CrossRef]

38. Lee, C.H.; Chang, Y.W.; Popuri, S.R.; Hung, C.E.; Liao, C.H.; Chang, J.E.; Chen, W.S. Recovery of Silicon, Copper and Aluminum from Scrap Silicon Wafers by Leaching and Precipitation. *Environ. Eng. Manag. J. (EEMJ)* **2018**, *17*, 561–568.

39. Ardente, F.; Latunussa, C.E.; Blengini, G.A. Resource efficient recovery of critical and precious metals from waste silicon PV panel recycling. *Waste Manag.* **2019**, *91*, 156–167. [CrossRef]

40. Berger, W.; Simon, F.G.; Weimann, K.; Alsema, E.A. A novel approach for the recycling of thin film photovoltaic modules. *Resour. Conserv. Recycl.* **2010**, *54*, 711–718. [CrossRef]

41. Mezei, A.; Ashbury, M.; Canizares, R.; Molnar, H.; Given, A.; Meader, K.; Squires, F.; Ojebuoboh, T. Jones, and W. Wang. Hydrometallurgical recycling of the semiconductor material from photovoltaic materials-Part one: Leaching. *Hydrometallurgy* **2008**, 209.

42. Hosseinipour, S.; Alamdari, E.K.; Sadeghi, N. Avrami Model for the Description of Nucleation and Growth of Tellurium During Cementation by Copper in the Sulfate Media. *Metall. Mater. Trans. B* **2023**, *54*, 2670–2679. [CrossRef]

43. Sasala, R.A.; Bohland, J.; Smigielski, K. Physical and chemical pathways for economic recycling of cadmium telluride thin-film photovoltaic modules. In Proceedings of the Twenty Fifth IEEE Photovoltaic Specialists Conference—1996, Washington, DC, USA, 13–17 May 1996.

44. Wang, W.; Fthenakis, V. Kinetics study on separation of cadmium from tellurium in acidic solution media using ion-exchange resins. *J. Hazard. Mater.* **2005**, *125*, 80–88. [CrossRef] [PubMed]

45. Zhang, T.; Dong, Z.; Qu, F.; Ding, F.; Peng, X.; Wang, H.; Gu, H. Removal of CdTe in acidic media by magnetic ion-exchange resin: A potential recycling methodology for cadmium telluride photovoltaic waste. *J. Hazard. Mater.* **2014**, *279*, 597–604. [CrossRef] [PubMed]

46. Simon, F.-G.; Holm, O.; Berger, W. Resource recovery from urban stock, the example of cadmium and tellurium from thin film module recycling. *Waste Manag.* **2013**, *33*, 942–947. [CrossRef]

47. Amato, A.; Beolchini, F. End-of-life CIGS photovoltaic panel: A source of secondary indium and gallium. *Prog. Photovolt. Res. Appl.* **2019**, *27*, 229–236. [CrossRef]

48. Zimmermann, Y.S.; Niewersch, C.; Lenz, M.; Kül, Z.; Corvini, P.F.X.; Schäffer, A.; Wintgens, T. Recycling of indium from CIGS photovoltaic cells: Potential of combining acid-resistant nanofiltration with liquid–liquid extraction. *Environ. Sci. Technol.* **2014**, *48*, 13412–13418. [CrossRef]

49. Kushiya, K.; Ohshita, M.; Tanaka, M. Development of recycling and reuse technologies for large-area Cu (InGa) Se/sub 2/-based thin-film modules. In Proceedings of the 3rd World Conference on Photovoltaic Energy Conversion, Osaka, Japan, 11–18 May 2003.

50. Palitzsch, W.; Loser, U. Systematic photovoltaic waste recycling. *Green* **2013**, *3*, 79–82. [CrossRef]

51. Menezes, S. Electrochemical solutions to some thin-film PV manufacturing issues. *Thin Solid Film.* **2000**, *361*, 278–282. [CrossRef]

52. Drinkard, W.F., Jr.; Long, M.O.; Goozner, R.E. Recycling of CIS Photovoltaic Waste. U.S. Patent 5,779,877, 14 July 1998.

53. Li, X.; Ma, B.; Hu, D.; Zhao, Q.; Chen, Y.; Wang, C. Efficient separation and purification of indium and gallium in spent Copper indium gallium diselenide (CIGS). *J. Clean. Prod.* **2022**, *339*, 130658. [CrossRef]

54. Hu, D.; Ma, B.; Li, X.; Lv, Y.; Chen, Y.; Wang, C. Innovative and sustainable separation and recovery of valuable metals in spent CIGS materials. *J. Clean. Prod.* **2022**, *350*, 131426. [CrossRef]

55. Nguyen, T.H.; Lee, M.S. A review on separation of gallium and indium from leach liquors by solvent extraction and ion exchange. *Miner. Process. Extr. Metall. Rev.* **2018**, *40*, 278–291. [CrossRef]

56. Kawatra, S.K. Waste Characterization and Treatment. *Min. Metall. Explor.* **1998**, *15*, 65. [CrossRef]

57. Yang, H.; Liu, J.; Yang, J. Leaching copper from shredded particles of waste printed circuit boards. *J. Hazard. Mater.* **2011**, *187*, 393–400. [CrossRef]

58. Silvas, F.P.C.; Jiménez Correa, M.M.; Caldas, M.P.K.; de Moraes, V.T.; Espinosa, D.C.R.; Tenório, J.A.S. Printed circuit board recycling: Physical processing and copper extraction by selective leaching. *Waste Manage.* **2015**, *46*, 503–510. [CrossRef]

59. Jha, M.K.; Lee, J.C.; Kumari, A.; Choubey, P.K.; Kumar, V.; Jeong, J. Pressure leaching of metals from waste printed circuit boards using sulfuric acid. *JOM* **2011**, *63*, 29–32. [CrossRef]

60. Ríos, G.; Ruiz, O.; Rius, M. Cruells, and Antonio Roca. Leaching of copper from a flash furnace dust using sulfuric acid. *Miner. Process. Extr. Metall. Rev.* **2022**, *43*, 411–421. [CrossRef]

61. Lawson, F.; Cheng, C.-Y.; Lee, L.S.Y. Leaching of copper sulphides and copper mattes in oxygenated chloride/sulphate leachants. *Miner. Procesing Extr. Metall. Rev.* **1992**, *8*, 183–203. [CrossRef]

62. Kavousi, M.; Sattari, A.; Alamdari, E.K.; Firozi, S. Selective separation of copper over solder alloy from waste printed circuit boards leach solution. *Waste Manage.* **2017**, *60*, 636–642. [CrossRef]

63. Agrawal, A.; Kumari, S.; Parveen, M.; Sahu, K.K. Exploitation of copper bleed stream for the extraction and recovery of copper and nickel by bis (2,4,4-trimethylpentyl) phosphinic acid. *Miner. Process. Extr. Metall. Rev.* **2012**, *33*, 339–351. [CrossRef]

64. Kumari, S.; Agrawal, A.; Bagchi, D.; Kumar, V.; Pandey, B.D. Synthesis of copper metal/salts from copper bleed solution of a copper plant. *Miner. Process. Extr. Metall. Rev.* **2006**, *27*, 159–175. [CrossRef]

65. Sahu, S.K.; Agrawal, B.D. Pandey, and Vinay Kumar. Recovery of copper, nickel and cobalt from the leach liquor of a sulphide concentrate by solvent extraction. *Miner. Eng.* **2004**, *17*, 949–951. [CrossRef]

66. Agrawal, A.; Kumari, M.K.; Manoj, B.D.; Kumar, P.V.; Bagchi, D. Seperation & Recovery of Copper & Nickel from Copper Bleed Stream by Solvent Extraction Route. In Proceedings of the International Symposium on Solvent Extraction, Bhubaneswar, India, 26–27 September 2022.

67. Kokes, H.; Morcali, M.; Acma, E. Dissolution of copper and iron from malachite ore and precipitation of copper sulfate pentahydrate by chemical process. *Eng. Sci. Technol. Int. J.* **2014**, *17*, 39–44. [CrossRef]

68. Deng, Z.; Oraby, E.; Eksteen, J. Sulfide precipitation of copper from alkaline glycine-cyanide solutions: Precipitate characterisation. *Miner. Eng.* **2020**, *145*, 106102. [CrossRef]

69. Nassef, E.; El-Taweel, Y.A. Removal of copper from wastewater by cementation from simulated leach liquors. *J. Chem. Eng. Process Technol.* **2015**, *6*, 1. [CrossRef]

70. Oghabi, H.; Haghshenas, D.F.; Firoozi, S. Selective separation of Cd from spent Ni-Cd battery using glycine as an eco-friendly leachant and its recovery as CdS nanoparticles. *Sep. Purif. Technol.* **2020**, *242*, 116832. [CrossRef]

71. Khodaei, H.; Haghshenas, D.F.; Firoozi, S. Selective leaching of zinc from carbonate source using glycine as an ecofriendly lixiviant. *Miner. Eng.* **2022**, *185*, 107680. [CrossRef]

72. Shin, D.; Ahn, J.; Lee, J. Kinetic study of copper leaching from chalcopyrite concentrate in alkaline glycine solution. *Hydrometallurgy* **2019**, *183*, 71–78. [CrossRef]

73. Eksteen, J.; Oraby, E.; Tanda, B. A conceptual process for copper extraction from chalcopyrite in alkaline glycinate solutions. *Miner. Eng.* **2017**, *108*, 53–66. [CrossRef]

74. Fiandra, V.; Sannino, L.; Andreozzi, C.; Corcelli, F.; Graditi, G. Silicon photovoltaic modules at end-of-life: Removal of polymeric layers and separation of materials. *Waste Manag.* **2019**, *87*, 97–107. [CrossRef]

75. Gasnot, L.; Decottignies, V.; Pauwels, J. Kinetics modelling of ethyl acetate oxidation in flame conditions. *Fuel* **2005**, *84*, 505–518. [CrossRef]

76. de Oliveira, L.S.S.; Lima, M.T.W.D.C.; Yamane, L.H.; Ribeiro Siman, R. Silver recovery from end-of-life photovoltaic panels. *Detritus* **2020**, *10*, 62–74. [CrossRef]

77. Rajahalme, J.; Perämäki, S.; Väisänen, A. Separation of palladium and silver from E-waste leachate: Effect of nitric acid concentration on adsorption to Thiol scavenger. *Chem. Eng. J. Adv.* **2022**, *10*, 100280. [CrossRef]

78. Bas, A.D.; Deveci, H.; Yazici, E.Y. Treatment of manufacturing scrap TV boards by nitric acid leaching. *Sep. Purif. Technol.* **2014**, *130*, 151–159. [CrossRef]

79. Aksu, S.; Doyle, F.M. Electrochemistry of copper in aqueous glycine solutions. *J. Electrochem. Soc.* **2001**, *148*, B51. [CrossRef]

80. Smith, R.M.; Martell, A.E. *Critical Stability Constants: Second Supplement*; Springer: Berlin/Heidelberg, Germany, 1989; Volume 6.

81. Agatino, C.; De Robertis, A.; De Stefano, C.; Gianguzza, A.; Patanè, G.; Rigano, C.; Sammartano, S. Thermodynamic parameters for the formation of glycine complexes with magnesium (II), calcium (II), lead (II), manganese (II), cobalt (II), nickel (II), zinc (II) and cadmium (II) at different temperatures and ionic strengths, with particular reference to natural fluid conditions. *Thermochim. Acta* **1995**, *255*, 109–141.

82. Horsch, W.G. Potentials of the zinc and cadmium electrodes. *J. Am. Chem. Soc.* **1919**, *41*, 1787–1800. [CrossRef]

83. Shen, Y.-S.; Ku, Y.; Wu, M.-H. The cementation of cadmium ion in aqueous solution by a zinc column test. *Sep. Sci. Technol.* **2003**, *38*, 3513–3534. [CrossRef]

84. Ku, Y.; Wu, M.-H.; Shen, Y.-S. A study on the cadmium removal from aqueous solutions by zinc cementation. *Sep. Sci. Technol.* **2002**, *37*, 571–590. [CrossRef]

85. Oraby, E.; Eksteen, J. Gold leaching in cyanide-starved copper solutions in the presence of glycine. *Hydrometallurgy* **2015**, *156*, 81–88. [CrossRef]

86. O'Connor, G.M.; Katerina Lepkova, J.J. Eksteen, and E. A. Oraby. Electrochemical behaviour of copper in alkaline glycine solutions. *Hydrometallurgy* **2018**, *181*, 221–229. [CrossRef]

87. Halpern, J.; Milants, H.; Wiles, D. Kinetics of the Dissolution of Copper in Oxygen-Containing Solutions of Various Chelating Agents. *J. Electrochem. Soc.* **1959**, *106*, 647. [CrossRef]

88. Oraby, E.; Eksteen, J. The selective leaching of copper from a gold–copper concentrate in glycine solutions. *Hydrometallurgy* **2014**, *150*, 14–19. [CrossRef]

89. Tanda, B.; Eksteen, J.; Oraby, E. An investigation into the leaching behaviour of copper oxide minerals in aqueous alkaline glycine solutions. *Hydrometallurgy* **2017**, *167*, 153–162. [CrossRef]

90. Barton, I.F.; Hiskey, J.B. Chalcopyrite leaching in novel lixiviants. *Hydrometallurgy* **2022**, *207*, 105775. [CrossRef]

91. Hao, J.; Wang, X.; Wang, Y.; Wu, Y.; Guo, F. Optimizing the leaching parameters and studying the kinetics of copper recovery from waste printed circuit boards. *ACS Omega* **2022**, *7*, 3689–3699. [CrossRef]

92. Han, Y.; Yi, X.; Wang, R.; Huang, J.; Chen, M.; Sun, Z.; Sun, S.; Shu, J. Copper extraction from waste printed circuit boards by glycine. *Sep. Purif. Technol.* **2020**, *253*, 117463. [CrossRef]

93. Li, H.; Oraby, E.; Eksteen, J. Extraction of copper and the co-leaching behaviour of other metals from waste printed circuit boards using alkaline glycine solutions. *Resour. Conserv. Recycl.* **2020**, *154*, 104624. [CrossRef]

94. Huang, Y.; Guo, H.; Zhang, C.; Liu, B.; Wang, L.; Peng, W.; Cao, Y.; Song, X.; Zhu, X. A novel method for the separation of zinc and cobalt from hazardous zinc–cobalt slag via an alkaline glycine solution. *Sep. Purif. Technol.* **2021**, *273*, 119009. [CrossRef]

95. Prasetyo, E.; Anderson, C.; Nurjaman, F.; Al Muttaqii, M.; Handoko, A.S.; Bahfie, F.; Rofiek Mufakhir, F. Monosodium glutamate as selective lixiviant for alkaline leaching of zinc and copper from electric arc furnace dust. *Metals* **2020**, *10*, 644. [CrossRef]

96. Sato, N.; Daimon, H.; Fujie, K. Decomposition of glycine in high temperature and high pressure water. *Kagaku Kogaku Ronbunshu* **2002**, *28*, 113–117. [CrossRef]

97. Li, J.; Zeng, X.; Chen, M.; Ogunseitan, O.A.; Stevels, A. "Control-Alt-Delete": Rebooting solutions for the e-waste problem. *Environ. Sci. Technol.* **2015**, *49*, 7095–7108. [CrossRef] [PubMed]

98. Nogueira, R.F.P.; Oliveira, M.C.; Paterlini, W.C. Simple and fast spectrophotometric determination of H_2O_2 in photo-Fenton reactions using metavanadate. *Talanta* **2005**, *66*, 86–91. [CrossRef] [PubMed]

99. Chernyaev, A.; Zou, Y.; Wilson, B.P.; Lundström, M. The interference of copper, iron and aluminum with hydrogen peroxide and its effects on reductive leaching of LiNi1/3Mn1/3Co1/3O$_2$. *Sep. Purif. Technol.* **2022**, *281*, 119903. [CrossRef]

100. Oraby, E.; Eksteen, J. The leaching of gold, silver and their alloys in alkaline glycine–peroxide solutions and their adsorption on carbon. *Hydrometallurgy* **2015**, *152*, 199–203. [CrossRef]

101. Paszkowicz, W.; Minikayev, P.; Piszora, D.; Trots, M.; Knapp, T. Wojciechowski, and R. Bacewicz. Thermal expansion of CuInSe 2 in the 11–1073 K range: An X-ray diffraction study. *Appl. Phys. A* **2014**, *116*, 767–780. [CrossRef]

102. Hariskos, D.; Bilger, D.; Braunger, M.R.; Schock, H.W. Investigations on the mechanism of the oxidation of Cu (In, Ga) Se2. In *Ternary and Multinary Compounds*; CRC Press: Boca Raton, FL, USA, 2020; pp. 707–710.

103. Balitskii, O.A.; Savchyn, P.P.; Lupshak, Y.; Fiyala, M. Peculiarities of (InxGa1− x) 2Se3 single crystal oxidation. *Mater. Lett.* **2001**, *51*, 27–31. [CrossRef]

104. Ho, T.-L. *Fiesers' Reagents for Organic Synthesis*; John Wiley & Sons: Hoboken, NJ, USA, 2016; Volume 28.

105. Swain, B.; Mishra, C.; Kang, L.; Park, K.S.; Lee, C.G.; Hong, H.S.; Park, J.L. Recycling of metal-organic chemical vapor deposition waste of GaN based power device and LED industry by acidic leaching: Process optimization and kinetics study. *J. Power Sources* **2015**, *281*, 265–271. [CrossRef]

106. Chen, W.-S.; Chung, Y.-F.; Tien, K.-W. Recovery of Gallium and Indium from Waste Light Emitting Diodes. *Resour. Recycl.* **2020**, *29*, 81–88. [CrossRef]

107. Rao, S.; Liu, Y.; Wang, D.; Cao, H.; Zhu, W.; Yang, R.; Duan, L.; Liu, Z. Pressure leaching of selenium and tellurium from scrap copper anode slimes in sulfuric acid-oxygen media. *J. Clean. Prod.* **2021**, *278*, 123989. [CrossRef]

108. McPhail, D. Thermodynamic properties of aqueous tellurium species between 25 and 350. *Geochim. Cosmochim. Acta* **1995**, *59*, 851–866.

109. Hosseinipour, S.; Alamdari, E.K.; Sadeghi, N. Selenium and Tellurium Separation: Copper Cementation Evaluation Using Response Surface Methodology. *Metals* **2022**, *12*, 1851. [CrossRef]